Application of Statistical Texture Features for Breast Tissue Density Classification

Kriti, Jitendra Virmani and Shruti Thakur

Abstract It has been strongly advocated that increase in density of breast tissue is strongly correlated with the risk of developing breast cancer. Accordingly change in breast tissue density pattern is taken seriously by radiologists. In typical cases, the breast tissue density patterns can be easily classified into fatty, fatty-glandular and dense glandular classes, but the differential diagnosis between atypical breast tissue density patterns from mammographic images is a daunting challenge even for the experienced radiologists due to overlap of the appearances of the density patterns. Therefore a CAD system for the classification of the different breast tissue density patterns from mammographic images is highly desirable. Accordingly in the present work, exhaustive experiments have been carried out to evaluate the performance of statistical features using PCA-kNN, PCA-PNN, PCA-SVM and PCA-SSVM based CAD system designs for two-class and three-class breast tissue density classification using mammographic images. It is observed that for two-class breast tissue density classification, the highest classification accuracy of 94.4 % is achieved using only the first 10 principal components (PCs) derived from statistical features with the SSVM classifier. For three-class breast tissue density classification, the highest classification accuracy of 86.3 % is achieved using only the first 4 PCs with SVM classifier.

Keywords Breast tissue density classification · Statistical features · Principal component analysis (PCA) · k-nearest neighbor (kNN) classifier · Probabilistic neural network (PNN) classifier · Support vector machine (SVM) classifier · Smooth support vector machine (SSVM) classifier

Kriti
Jaypee University of Information Technology, Solan, Himachal Pradesh, India
e-mail: kriti.23gm@gmail.com

J. Virmani (✉)
Thapar University, Patiala, Punjab, India
e-mail: jitendra.virmani@gmail.com

S. Thakur
Department of Radiology, IGMC, Shimla, Himachal Pradesh, India
e-mail: tshruti878@yahoo.in

A.I. Awad and M. Hassaballah (eds.), *Image Feature Detectors and Descriptors*,
Studies in Computational Intelligence 630, DOI 10.1007/978-3-319-28854-3_16

1 Introduction

Cancer comes under a class of diseases that are characterized by uncontrolled growth of cells resulting in formation of tissue masses called tumors at any location in the body [1]. The malignant tumor can destroy other healthy tissues in the body and often travels to other parts of the body to form new tumors. This process of invasion and destruction of healthy tissues is called metastasis [2]. Breast cancer is the type of cancer that develops form breast cells. It is considered to be a major health problem nowadays and is the most common form of cancer found in women [3]. For the women in United Kingdom, the lifetime risk of being diagnosed with breast cancer is 1 in 8 [4]. The study in [5] reported 1.67 million new incidences of breast cancer worldwide in the year 2012. There are various risk factors associated with cancer development: (*a*) Age, (*b*) History of breast cancer, (*c*) Formation of certain lumps in the breasts (*d*) Higher breast density, (*e*) Obesity, (*f*) Alcohol consumption, (*g*) Cosmetic implants.

It has been strongly advocated by many researchers in their study that high breast density is strongly correlated with the risk of developing breast cancer [6–14]. The association between increased breast density and breast cancer risk can be explained on the basis of effects due to the hormones mitogens and mutagens. The size of the cell population in the breast and cell proliferation is affected by mitogens while the likelihood of damage to these cells is due to mutagens. Due to increased cell population, there is an increase in reactive oxygen species (ROS) production and lipid peroxidation. The products of lipid peroxidation; malondialdehyde (MDA) and isoprostanes catalyze the proliferation of cells [15].

Even though breast cancer is considered to be a fatal disease with a high mortality rate, the chances of survival are improved significantly if it can be detected at an early stage. Various imaging modalities like ultrasound, MRI, computerized tomography, etc. can be used for diagnosis of breast abnormalities but mammography is considered to be the best choice for detection due to its higher sensitivity [16–23]. Mammography is an X-ray imaging technique used to detect the breast abnormalities. Mammograms display the adipose (fatty) and fibroglandular tissues of the breast along with the present abnormalities.

On the basis of density, breast tissue can be classified into the following categories:

(a) *Fatty (F)/Dense (D) (Two-class classification)*
(b) *Fatty (F)/Fatty-glandular (FG)/Dense-glandular (DG) (Three-class classification)*
(c) *Almost entirely fatty (B-I)/Some fibro-glandular tissue (B-II)/Heterogeneously dense breast (B-III)/Extremely dense breast (B-IV) (Four-class BI-RADS classification)*

The typical fatty tissue being translucent to X-rays appears dark on a mammogram where as the dense tissues appear bright on the mammograms. The fatty-glandular breast tissue is an intermediate stage between fatty and dense tissues therefore a typical fatty-glandular breast tissue appears dark with some bright streaks on the

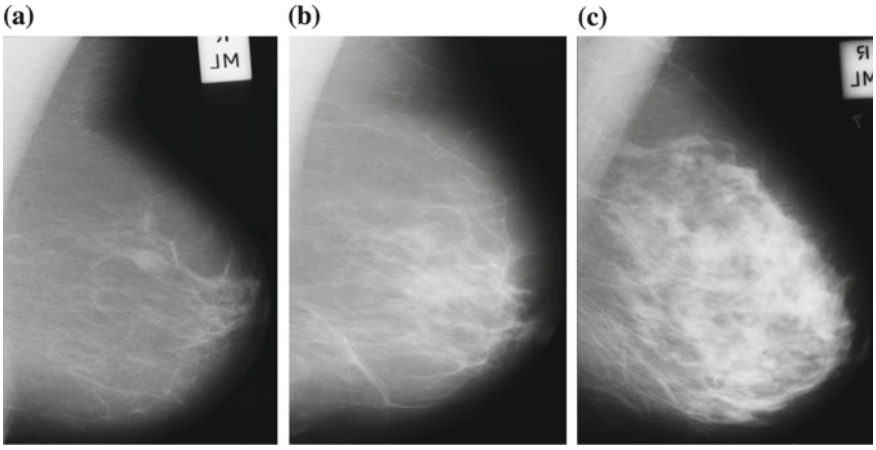

Fig. 1 Sample mammographic images depicting typical cases. **a** Typical fatty tissue 'mdb012'. **b** Typical fatty-glandular tissue 'mdb014'. **c** Typical dense-glandular tissue 'mdb108'

mammogram. The mammographic appearances of the typical breast tissues based on density are depicted in Fig. 1.

The discrimination between different density patterns by visual analysis is highly subjective and depends on the experience of the radiologist. The participating radiologist i.e. one of the co-author of this work, opined that, in case of atypical cases where there is a high overlap in appearances of the different density patterns, a clear discrimination cannot be made by visual analysis easily. The sample mammographic images depicting the atypical cases are shown in Fig. 2.

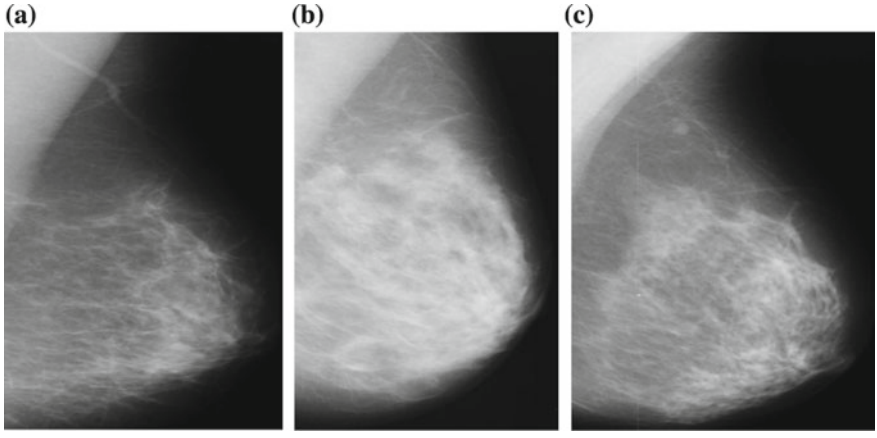

Fig. 2 Sample mammographic images depicting atypical cases **a** Atypical fatty tissue 'mdb088'. **b** Atypical fatty-glandular tissue 'mdb030'. **c** Atypical dense-glandular tissue 'mdb100'

In order to correctly identify and analyze these atypical cases various computer aided diagnostic (CAD) systems have been developed for breast tissue density classification. These proposed CAD systems can be categorized as: (*a*) CAD system designs based on segmented breast tissue versus CAD system designs based on Regions of Interest (ROIs). (*b*) CAD system designs for two class classification (fatty/dense) versus CAD system designs for three class classification (fatty/fatty-glandular/dense-glandular) versus CAD system designs for four class classification based on BI-RADS (B-I: almost entirely fatty/B-II: some fibro-glandular tissue/B-III: heterogeneously dense breast/B-IV: extremely dense breast). (*c*) CAD system designs using standard benchmark dataset (Mammographic image analysis society (MIAS), Digital database of screening mammograms (DDSM), Oxford, Nijmegen) versus CAD system designs using data collected by individual research groups. A brief description of the related studies is given in Tables 1, 2 and 3.

From the above tables, it can be observed that most of the researchers have used a subset of MIAS and DDSM databases and have worked on the segmented breast tissue. It is also observed that only a few studies report CAD systems based on ROIs

Table 1 Summary of studies carried out for two-class breast tissue density classification

Investigators	Dataset description				
	Database	No. of images	ROI size	Classifier	OCA (%)
Miller and Astley [24]	Collected by investigator	40	SBT	Bayesian	80.0
Bovis and Singh [25]	DDSM (SBMD)	377	SBT	ANN	96.7
Castella et al. [26]	Collected by investigator	352	256 × 256	LDA	90.0
Oliver et al. [27]	MIAS (SBMD)	322	SBT	Bayesian	91.0
	DDSM (SBMD)	831			84.0
Mustra et al. [28]	MIAS (SBMD)	322	512 × 384	Naïve Bayesian	91.6
	KBD-FER (Collected by investigator)	144		IB1	97.2
Sharma and Singh [29]	MIAS (SBMD)	322	200 × 200	SMO-SVM	96.4
Sharma and Singh [30]	MIAS (SBMD)	212	200 × 200	kNN	97.2
Kriti et al. [31]	MIAS (SBMD)	322	200 × 200	SVM	94.4
Virmani et al. [32]	MIAS (SBMD)	322	200 × 200	kNN	96.2

Note SBMD Standard benchmark database. *SBT* Segmented breast tissue. *OCA* Overall Classification Accuracy

Table 2 Summary of studies carried out for three-class breast tissue density classification

Investigators	Dataset description				
	Database	No. of images	ROI size	Classifier	OCA (%)
Blot and Zwiggelaar [33]	MIAS (SBMD)	265	SBT	kNN	63.0
Bosch et al. [34]	MIAS (SBMD)	322	SBT	SVM	91.3
Muhimmah and Zwiggelaar [35]	MIAS (SBMD)	321	SBT	DAG-SVM	77.5
Subashini et al. [36]	MIAS (SBMD)	43	SBT	SVM	95.4
Tzikopoulos et al. [37]	MIAS (SBMD)	322	SBT	SVM	84.4
Li [38]	MIAS (SBMD)	42	SBT	KSFD	94.4
Mustra et al. [28]	MIAS (SBMD)	322	512 × 384	IB1	82.0
Silva and Menotti [39]	MIAS (SBMD)	320	300 × 300	SVM	77.1

Note SBMD Standard benchmark database. *SBT* Segmented breast tissue. *OCA* Overall Classification Accuracy

Table 3 Summary of studies carried out for four-class breast tissue density classification

Investigators	Dataset description				
	Database	No. of images	ROI size	Classifier	OCA (%)
Karssemeijer [40]	Nijmegen (SBMD)	615	SBT	kNN	80.0
Wang et al. [41]	Collected by investigator	195	SBT	NN	71.0
Petroudi et al. [42]	Oxford (SBMD)	132	SBT	Nearest neighbor	76.0
Oliver et al. [43]	DDSM (SBMD)	300	SBT	kNN+ID3	47.0
Bosch et al. [34]	MIAS (SBMD)	322	SBT	SVM	95.4
	DDSM (SBMD)	500			84.7
Castella et al. [26]	Collected by investigator	352	256 × 256	LDA	83.0
Oliver et al. [27]	MIAS (SBMD)	322	SBT	Bayesian	86.0
	DDSM (SBMD)	831			77.0
Mustra et al. [28]	MIAS (SBMD)	322	512 × 384	IB1	79.2
	KBD-FER (collected by investigator)	144			76.4

Note SBMD Standard benchmark database. *SBT* Segmented breast tissue. *OCA* Overall Classification Accuracy

extracted from the breast [26, 28–32, 39] even though it has been shown that the ROIs extracted from the center of the breast result in highest performance as this region of the breast is densest and extraction of ROIs also eliminates an extra step of

preprocessing included in obtaining the segmented breast tissue for pectoral muscle removal [44].

The chapter is organized into three sections. Section 2 presents the methodology adopted for present work, i.e. (*a*) description of the dataset on which the work has been carried out (*b*) description of texture features extracted from each ROI image and (*c*) description of the classification module. Section 3 describes the various experiments carried out in the present work for two-class and three-class breast tissue density classification using statistical texture features. Finally, Sect. 4 reports the conclusions drawn from the exhaustive experiments carried out in the present work for two-class and three-class breast tissue density classification.

2 Methodology

2.1 Dataset Description

In the present work a publicly available database, mini-MIAS has been used. This database consists of the Medio Lateral Oblique (MLO) views of both the breasts of 161 women i.e. a total of 322 mammographic images. These images are selected from the UK National Breast Screening Programme and were digitized using The Joyce-Loebl scanning microdensitometer. The images in the database are categorized into three categories as per their density namely fatty (106 images), fatty-glandular (104 images) and dense-glandular (112 images). Each image in the database is of size 1024 $\times$ 1024 pixels, with 256 gray scale tones and a horizontal and vertical resolution of 96 dpi. The database also includes location of abnormality, the radius of the circle enclosing the abnormality, its severity and nature of the tissue [45]. In the present work CAD system designs have been proposed for (*a*) two-class breast tissue density classification i.e. (fatty and dense class) and (*b*) three-class breast tissue density classification i.e. (fatty, fatty-glandular and dense-glandular classes). For implementing CAD systems for two-class breast tissue density classification, the fatty-glandular and dense-glandular classes are combined and considered as dense class resulting in 106 mammograms belonging to fatty class and 216 mammograms belonging to dense class. The description of the dataset, used for two-class and three-class CAD system designs is shown in Fig. 3.

2.2 Region of Interest (ROI) Selection

The ROI size is selected carefully considering the fact that it should provide a good population of pixels for computing texture features [44]. Different ROI sizes that have been selected in the literature for classification are 256 $\times$ 256 pixels [26], 512 $\times$ 384 pixels [28], 200 $\times$ 200 pixels [29–32] and 300 $\times$ 300 pixels [39]. Other

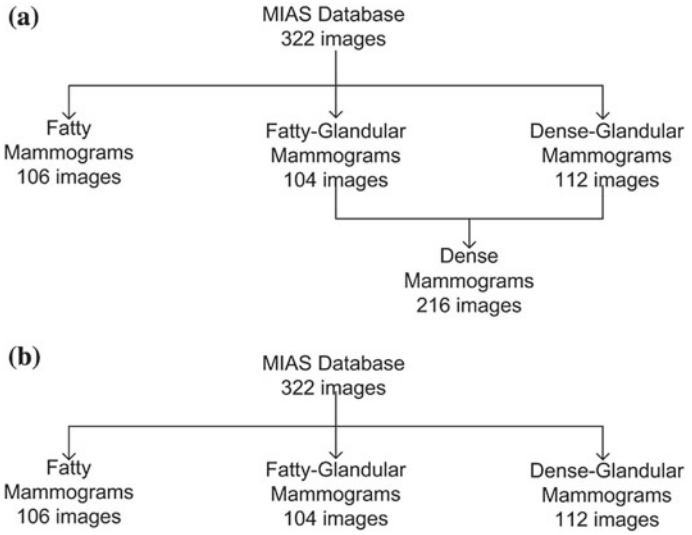

Fig. 3 Dataset description. **a** Two-class breast tissue density classification. **b** Three-class breast tissue density classification

researchers have pre-processed the mammograms by removal of the pectoral muscle and the background using segmented breast tissue for feature extraction [24, 25, 27, 33–38, 40–43]. The participating radiologist, one of the coauthors opined that for accessing the breast tissue density patterns, visual analysis of texture patterns of the center of the breast tissue is carried out during routine practice. Accordingly, for the present work, ROIs of size 200 × 200 pixels are manually extracted from each mammogram. The ROIs are selected from the center of the breast tissue as it has also been asserted by many researchers in their research that the center region of the breast tissue is the densest region and selecting ROI from this part of the breast results in highest performance of the proposed algorithms [29–32, 44]. The selection and extraction of ROI from the breast tissue is shown in Fig. 4.

The sample images of ROIs extracted from the mammographic images are shown in Fig. 5.

2.3 Experimental Workflow for Design of CAD System for Two-Class and Three-Class Breast Tissue Density Classification

With the advancement in computer technology and artificial intelligence techniques there has been a substantial increase in the opportunities for researchers to investigate the potential of CAD systems for texture analysis and tissue characterization of

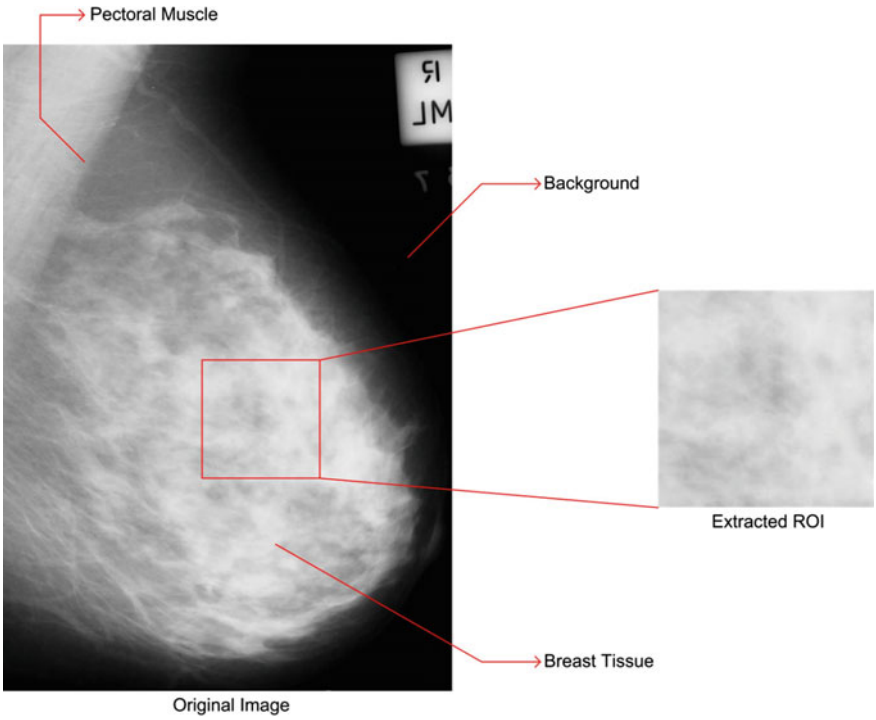

Fig. 4 Sample mammographic image with ROI marked

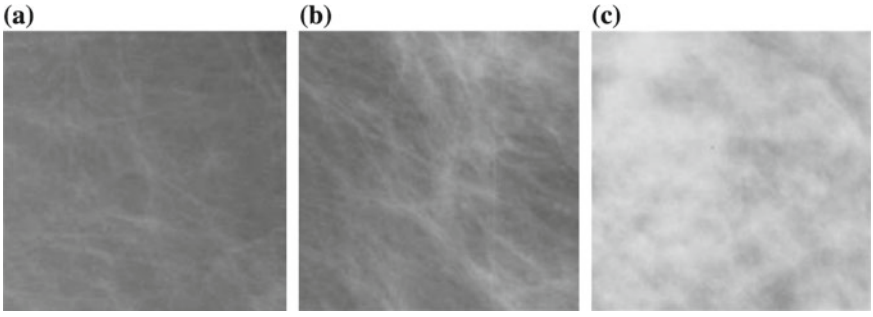

Fig. 5 Sample ROI images. **a** Fatty tissue 'mdb012', **b** Fatty-glandular tissue 'mdb014', **c** Dense-glandular tissue 'mdb108'

radiological images [46–58]. Tissue characterization refers to quantitative analysis of the tissue imaging features resulting in accurate distinction between different types of tissues. Thus, the result of tissue characterization is interpreted using numerical values. The overall aim of developing a computerized tissue characterization system is to provide additional diagnostic information about the underlying tissue which cannot be captured by visual inspection of medical images.

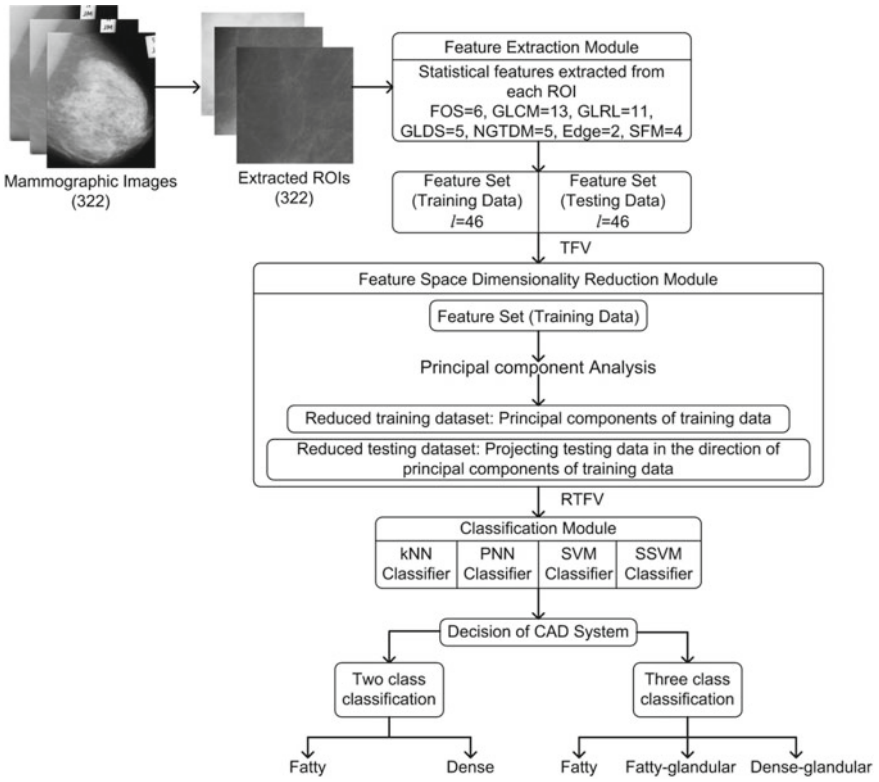

Fig. 6 Experimental workflow for design of CAD systems for two-class and three class breast tissue density classification

The CAD systems are used in the medical imaging as a second opinion tool for the radiologists to gain confidence in their diagnosis. In radiology, CAD systems improve the diagnostic accuracy for medical image interpretation helping the radiologists in detecting the lesions present in the images which might be missed by them.

In general, CAD system design consists of feature extraction module, feature space dimensionality reduction module and classification module. For implementing the proposed CAD system design for breast density classification, 322 ROIs are extracted from 322 images of the MIAS database. The block diagram of experimental workflow followed in the present work is shown in Fig. 6.

For the present CAD system design, ROIs are manually extracted from the mammograms of the MIAS database. In feature extraction module statistical features are extracted from the ROIs. In feature space dimensionality reduction module, PCA is applied to the feature set (training data) to derive its principal components (PCs). The reduced testing dataset is obtained by projecting the data points of feature set (testing data) in the direction of the PCs of feature set (training data). In feature classification module 4 classifiers i.e. k-nearest neighbor (kNN) classifier, proba-

bilistic neural network (PNN) classifier, support vector machine (SVM) classifier and smooth support vector machine (SSVM) classifier are used for the classification task. These classifiers are trained and tested using the reduced texture feature vectors (RTFVs) i.e. set of optimal PCs obtained after applying PCA.

2.3.1 Feature Extraction Module

The feature extraction is the process used to transform the visually extractable and non-extractable features into mathematical descriptors. These descriptors are either shape-based (morphological features) or intensity distribution based (textural features). There are a variety of methods to extract the textural features including statistical, signal processing based and transform domain methods. The different methods of feature extraction are depicted in Fig. 7.

In the present work, the statistical methods are used to extract the texture features from an image based on the gray level intensities of the pixels of that image.

First Order Statistics (FOS) Features

Six features namely average gray level, standard deviation, smoothness, kurtosis and entropy are computed for each ROI [59].

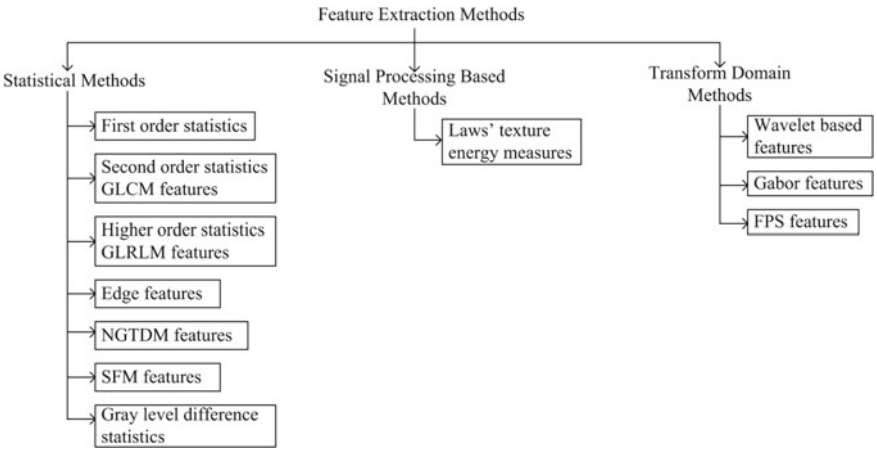

Fig. 7 Different feature extraction methods. **Note**: GLCM: Gray level co-occurrence matrix, GLRLM: Gray level run length matrix, NGTDM: Neighborhood gray tone difference matrix, SFM: Statistical feature matrix, FPS: Fourier power spectrum

Second Order Statistics-Gray Level Co-occurrence Matrix (GLCM) Features

To derive the statistical texture features from GLCM, spatial relationship between two pixels is considered. The GLCM tabulates the number of times the different combinations of pixel pairs of a specific gray level occur in an image for various directions $\theta = 0°, 45°, 90°, 135°$ and different distances d = 1, 2, 3 etc. A total of 13 GLCM features namely angular second moment (ASM), correlation, contrast, variance, inverse difference moment, sum average, sum variance, difference variance, entropy, sum entropy, difference entropy, information measures of correlation-1 and information measures of correlation-2 are computed from each ROI [60–62].

Higher Order Statistics-Gray Level Run Length Matrix (GLRLM) Features

To derive the statistical texture features from the GLRLM, spatial relationship between more than two pixels is considered. In a given direction, GLRLM measures the number of times there are runs of consecutive pixels with the same value. Total of 11 GLRLM features namely short run emphasis, long run emphasis, low gray level run emphasis, high gray level run emphasis, short run low gray level emphasis, short run high gray level emphasis, long run low gray level emphasis, long run high gray level emphasis, gray level non uniformity, run length non-uniformity and run percentage are computed from each ROI [63, 64].

Edge Features (Absolute Gradient)

The edges in an image contain more information about the texture than other parts of the image. The gradient of an image measures the spatial variation of gray levels across an image. At an edge, there is an abrupt change in gray level of the image. If the gray level variation at some point is abrupt then that point is said to have a high gradient and if the variation is smooth the point is at low gradient. Absolute gradient is used to judge whether the gray level variation in an image is smooth or abrupt. The texture features computed are absolute gradient mean and absolute gradient variance [65].

Neighborhood Gray Tone Difference Matrix (NGTDM) Features

NGTDM represents a difference in grayscale between pixels with a certain gray scale and the neighboring pixels. Features extracted from NGTDM are: coarseness, contrast, business, complexity and strength [26, 66].

Statistical Feature Matrix (SFM) Features

SFM is used to measure the statistical properties of pixels at several distances within an image. The features computed from SFM are coarseness, contrast, periodicity and roughness.

Gray Level Difference Statistics (GLDS)

These features are based on the co-occurrence of a pixel pair having a given absolute difference in gray-levels separated by a particular distance. The extracted features are: homogeneity, contrast, energy, entropy and mean [67, 68].

2.3.2 Feature Space Dimensionality Reduction Module

The texture feature vector (TFV) formed after computing the texture features in the feature extraction module may contain some redundant and correlated features which when used in the classification task can degrade the performance of the proposed CAD system. These redundant features give no extra information that proves to be helpful in discriminating the textural changes exhibited by different density patterns. Hence, to remove these redundant features and obtain the optimal attributes for the classification task, PCA is employed [69–71]. Steps used in the PCA algorithm are:

(1) Normalize each feature in dataset to zero mean and unity variance.
(2) Obtain co-variance matrix of the training dataset.
(3) Obtain Eigen values and Eigen vectors from the co-variance matrix. Eigen vectors give the directions of the PCs.
(4) Project the data points in testing dataset in the direction of the PCs of training dataset.

The obtained PCs are uncorrelated to each other and the 1st PC has the largest possible variance out of all the successive PCs. The optimal number of PCs is determined by performing repeated experiments by going through first few PCs i.e. by first considering the first two PCs, then first three PCs and so on, and evaluating the performance of the classifier for each experiment.

2.3.3 Feature Classification Module

Classification is a machine learning technique, used to predict the class membership of unknown data instances based on the training set of data containing instances whose class membership is known. In this module, different classifiers like kNN, PNN, SVM and SSVM are employed to classify the unknown testing instances of mammographic images. The extracted features are normalized in the range [0, 1]

by using min-max normalization procedure to avoid any bias caused by unbalanced feature values. The different classifiers employed in the present work are described as below:

k-Nearest Neighbor (kNN) Classifier

The kNN classifier is based on the idea of estimating the class of an unknown instance from its neighbors. It tries to cluster the instances of feature vector into disjoint classes with an assumption that instances of feature vector lying close to each other in feature space represent instances belonging to the same class. The class of an unknown instance in testing dataset is selected to be the class of majority of instances among its k-nearest neighbors in the training dataset. The advantage of kNN is its ability to deal with multiple class problems and is robust to noisy data as it averages the k-nearest neighbors [71–74]. Euclidean distance is used as a distance metric. The classification performance of kNN classifier depends on the value of k. In the present work, the optimal value of k and number of PCs to be retained is determined by performing repeated experiments for the values of $k \in \{1, 2, \ldots, 9, 10\}$ and number of PCs $\in \{1, 2, \ldots, 14, 15\}$. If same accuracy is obtained for more than one value of k, smallest value of k is used to obtain the result.

Probabilistic Neural Network (PNN) Classifier

The PNN is a supervised feed-forward neural network used for estimating the probability of class membership [75–77]. The architecture of PNN has four layers: input layer, pattern layer, summation layer and output layer. Primitive values are passed to the 'n' neurons in the input unit. Values from the input unit are passed to the hidden units in the pattern layer where responses for each unit are calculated. There are 'p' number of neurons in the pattern layer, one for each class. In the pattern layer a probability density function for each class is defined based on the training dataset and optimized kernel width parameter. Values of each hidden unit are summed in the summation layer to get response in each category. Maximum response is taken from all categories in the decision layer to get the class of the unknown instance. The optimal choice of spread parameter (Sp) i.e. the kernel width parameter is critical for the classification using PNN. In the present work, the optimal values used for Sp and optimal number of PCs to design a PNN classifier are determined by performing repeated experiments for values of Sp $\in \{1, 2, \ldots, 9, 10\}$ and number of PCs $\in \{1, 2, \ldots, 14, 15\}$.

Support Vector Machine (SVM) Classifier

The SVM classifier belongs to a class of supervised machine learning algorithms. It is based on the concept of decision planes that define the decision boundary.

In SVM, kernel functions are used to map the non-linear training data from input space to a high dimensionality feature space. Some common kernels are polynomial, Gaussian radial basis function and sigmoid. In the present work, SVM classifier is implemented using LibSVM library [78] and the performance of the Gaussian Radial Basis Function kernel is investigated. The critical step for obtaining a good generalization performance is the correct choice of regularization parameter C and kernel parameter γ. The regularization parameter C tries to maximize the margin while keeping the training error low. In the present work, ten-fold cross validation is carried out on the training data, for each combination of (C, γ) such that, C $\in \{2^{-4}, 2^{-3}, \ldots, 2^{15}\}$ and $\gamma \in \{2^{-12}, 2^{-11}, \ldots, 2^{4}\}$. This grid search procedure in parameter space gives the optimum values of C and γ for which training accuracy is maximum [79–83].

Smooth Support Vector Machine (SSVM) Classifier

To solve important mathematical problems related to programming, smoothing methods are extensively used. SSVM works on the idea of smooth unconstrained optimization reformulation based on the traditional quadratic program which is associated with SVM [84, 85]. For implementing SSVM classifier, the SSVM toolbox developed by Laboratory of Data Science and Machine Intelligence, Taiwan was used [86]. Similar to SVM implementation in case of SSVM also, ten-fold cross validation is carried out on training data for each combination of (C, γ) such that, C $\in \{2^{-4}, 2^{-3}, \ldots, 2^{15}\}$ and $\gamma \in \{2^{-12}, 2^{-11}, \ldots, 2^{4}\}$. This grid search procedure in parameter space gives the optimum values of C and γ for which training accuracy is maximum.

Classifier Performance Evaluation Criteria

The performance of the CAD system for two-class and three class breast tissue density classification can be measured using overall classification accuracy (OCA) and individual class accuracy (ICA). These values can be calculated using the confusion matrix (CM).

$$\text{OCA} = \frac{\Sigma \text{ No. of correctly classified images of each class}}{\text{Total images in testing dataset}} \tag{1}$$

$$\text{ICA} = \frac{\text{No. of correctly classified images of one class}}{\text{Total no. of images in the testing dataset for that class}} \tag{2}$$

3 Results

Rigorous experimentation was carried out in the present work to characterize the mammographic images as per breast tissue density. The experiments carried out in the present work are described in Tables 4 and 5, respectively for two-class and three-class breast tissue density classification.

3.1 Experiments Carried Out for Two-Class Breast Tissue Density Classification

3.1.1 Experiment 1: To Obtain the Classification Performance of Statistical Features for Two-Class Breast Tissue Density Classification Using kNN, PNN, SVM and SSVM Classifiers

In this experiment, classification performance of TFV containing different statistical features is evaluated for two-class breast tissue density classification using different classifiers. The results of the experiment are shown in Table 6. It can be observed from the table that for statistical features, the overall classification accuracy of 92.5, 91.3, 90.6 and 92.5 % is achieved using kNN, PNN, SVM and SSVM classifiers, respectively. It can also be observed that the highest in individual class accuracy for fatty class is 83.0 % with SSVM classifier and highest individual class accuracy for dense class is 100 %, using PNN classifier. Out of total 161 testing instances, 12 instances (12/161) are misclassified in case of kNN, 14 instances (14/161) are misclassified in case of PNN, 16 instances (16/161) are misclassified in case of SVM and 12 instances (12/161) are misclassified in case of SSVM classifier.

Table 4 Description of experiments carried out for two-class breast tissue density classification

Experiment 1	To obtain the classification performance of statistical features for two-class breast tissue density classification using kNN, PNN, SVM and SSVM classifiers
Experiment 2	To obtain the classification performance of statistical features for two-class breast tissue density classification using PCA-kNN, PCA-PNN, PCA-SVM and PCA-SSVM classifiers

Table 5 Description of experiments carried out for three-class breast tissue density classification

Experiment 1	To obtain the classification performance of statistical features for three-class breast tissue density classification using kNN, PNN, SVM and SSVM classifiers
Experiment 2	To obtain the classification performance of statistical features for three-class breast tissue density classification using PCA-kNN, PCA-PNN, PCA-SVM and PCA-SSVM classifiers

Table 6 Classification performance of statistical features using kNN, PNN, SVM and SSVM classifiers for two-class breast tissue density classification

Classifier	CM			OCA (%)	ICA_F (%)	ICA_D (%)
		F	D			
kNN	F	43	10	*92.5*	81.1	98.1
	D	2	106			
PNN	F	39	14	91.3	73.5	100
	D	0	108			
SVM	F	41	12	90.6	77.3	96.2
	D	4	104			
SSVM	F	44	9	*92.5*	83.0	97.2
	D	3	105			

Note CM Confusion matrix, *F* Fatty class, *D* Dense class, *OCA* Overall classification accuracy, ICA_F Individual class accuracy for fatty class, ICA_D Individual class accuracy for dense class

3.1.2 Experiment 2: To Obtain the Classification Performance of Statistical Features for Two-Class Breast Tissue Density Classification Using PCA-kNN, PCA-PNN, PCA-SVM and PCA-SSVM Classifiers

In this experiment, classification performance of reduced texture feature vector (RTFV) derived by applying PCA to TFV containing different statistical features is evaluated for two-class breast tissue density classification using different classifiers. The results are shown in Table 7.

It can be observed from the table that the overall classification values of 91.9, 91.3, 93.7 and 94.4 % have been achieved using the PCA-kNN, PCA-PNN, PCA-SVM

Table 7 Classification performance of statistical features using PCA-kNN, PCA-PNN, PCA-SVM and PCA-SSVM classifiers for two-class breast tissue density classification

Classifier	l	CM			OCA (%)	ICA_F (%)	ICA_D (%)
			F	D			
kNN	6	F	43	10	91.9	81.1	97.2
		D	3	105			
PNN	4	F	39	14	91.3	73.5	100
		D	0	108			
SVM	7	F	43	10	93.7	81.1	100
		D	0	108			
SSVM	10	F	47	6	*94.4*	88.6	97.2
		D	3	105			

Note l No. of PCs, *CM* Confusion matrix, *F* Fatty class, *D* Dense class, *OCA* Overall classification accuracy, ICA_F Individual class accuracy for fatty class, ICA_D Individual class accuracy for dense class

and PCA-SSVM classifiers, respectively. It can also be observed that the highest individual class accuracy for fatty class is 88.6 % using PCA-SSVM classifier and that for dense class is 100 % using PCA-PNN and PCA-SVM classifiers. Out of total 161 testing instances, 13 instances (13/161) are misclassified in case of PCA-kNN, 14 instances (14/161) are misclassified in case of PCA-PNN, 10 instances (10/161) are misclassified in case of PCA-SVM and 9 instances (9/161) are misclassified in case of PCA-SSVM classifier.

From the results obtained from the above experiments, it can be observed that for two-class breast tissue density, PCA-SSVM classifier achieves highest classification accuracy of 94.4 % using first 10 PCs.

3.2 Experiments Carried Out for Three-Class Breast Tissue Density Classification

3.2.1 Experiment 1: To Obtain the Classification Performance of Statistical Features for Three-Class Breast Tissue Density Classification Using kNN, PNN, SVM and SSVM Classifiers

In this experiment, the classification performance of TFV containing different statistical features is evaluated for three-class breast tissue density classification using different classifiers. The results are shown in Table 8.

It can be observed from the table that the overall classification accuracy of 86.9, 85.0, 83.8 and 82.6 % is achieved using kNN, PNN, SVM and SSVM classifiers, respectively. The highest individual class accuracy for fatty class is 94.3 % using SVM classifier, for fatty-glandular class the highest individual class accuracy achieved is 88.4 % using SSVM classifier and for the dense-glandular class, highest individual class accuracy achieved is 96.4 % using kNN classifier. Out of total 161 testing instances, 21 instances (21/161) are misclassified in case of kNN, 24 instances (24/161) are misclassified in case of PNN, 26 instances (26/161) are misclassified in case of SVM and 28 instances (28/161) are misclassified in case of SSVM classifier.

3.2.2 Experiment 2: To Obtain the Classification Performance of Statistical Features for Three-Class Breast Tissue Density Classification Using PCA-kNN, PCA-PNN, PCA-SVM and PCA-SSVM Classifiers

In this experiment, the classification performance of RTFV derived by applying PCA to TFV containing different statistical features is evaluated for three-class breast tissue density classification using different classifiers. The results are shown in Table 9. It can be observed from the table that the overall classification of 85.0, 84.4, 86.3 and 85.0 % is achieved using PCA-kNN, PCA-PNN, PCA-SVM and PCA-SSVM

Table 8 Classification performance of statistical features using kNN, PNN, SVM and SSVM classifiers for three-class breast tissue density classification

Classifier	CM				OCA (%)	ICA_F (%)	ICA_{FG} (%)	ICA_{DG} (%)
		F	FG	DG				
kNN	F	46	2	5	*86.9*	86.7	76.9	96.4
	FG	2	40	10				
	DG	0	2	54				
PNN	F	41	8	4	85.0	77.3	82.6	94.6
	FG	1	43	8				
	DG	0	3	53				
SVM	F	50	3	0	83.8	94.3	67.3	89.2
	FG	12	35	5				
	DG	1	5	50				
SSVM	F	39	11	3	82.6	73.5	88.4	85.7
	FG	3	46	3				
	DG	1	7	48				

Note CM Confusion matrix, *F* Fatty class, *FG* Fatty–glandular class, *DG* Dense-glandular class, *OCA* Overall classification accuracy, ICA_F Individual class accuracy for fatty class, ICA_{FG} Individual class accuracy for fatty-glandular class, ICA_{DG} Individual class accuracy for dense-glandular class

Table 9 Classification performance of statistical features using PCA-kNN, PCA-PNN, PCA-SVM and PCA-SSVM classifiers for three-class breast tissue density classification

Classifier	*l*	CM				OCA (%)	ICA_F (%)	ICA_{FG} (%)	ICA_{DG} (%)
			F	FG	DG				
kNN	9	F	44	4	5	85.0	83.0	73.0	98.2
		FG	3	38	11				
		DG	1	0	55				
PNN	6	F	43	6	4	84.4	81.1	84.6	87.5
		FG	1	44	7				
		DG	0	7	49				
SVM	4	F	47	4	2	*86.3*	88.6	76.9	92.8
		FG	6	40	6				
		DG	0	4	52				
SSVM	5	F	43	9	1	85.0	81.1	84.6	89.2
		FG	4	44	4				
		DG	0	6	50				

Note l Optimal number of PCs, *CM* Confusion matrix, *F* Fatty class, *FG* Fatty–glandular class, *DG* Dense-glandular class, *OCA* Overall classification accuracy, ICA_F Individual class accuracy for fatty class, ICA_{FG} Individual class accuracy for fatty-glandular class, ICA_{DG} Individual class accuracy for dense-glandular class

classifiers, respectively. The highest individual class accuracy for fatty class is 88.6 % using PCA-SVM classifier, for fatty-glandular class the highest individual class accuracy achieved is 84.6 % using PCA-PNN and PCA-SSVM classifiers and for the dense-glandular class, highest individual class accuracy achieved is 98.2 % using PCA-kNN classifier. Out of total 161 testing instances, 24 instances (24/161) are misclassified in case of PCA-kNN, 25 instances (25/161) are misclassified in case of PCA-PNN, 22 instances (22/161) are misclassified in case of PCA-SVM and 24 instances (24/161) are misclassified in case of PCA-SSVM classifier.

For three-class breast tissue density classification, it can be observed from the above experiments that highest classification accuracy of 86.9 % is achieved using the kNN classifier, however it should also be noted that PCA-SVM classifier achieves the highest classification accuracy of 86.3 % by using only the first 4 PCs obtained by applying PCA to the TFV of statistical features. Thus CAD system design based on PCA-SVM classifier can be considered to be the best choice for three-class breast tissue density classification.

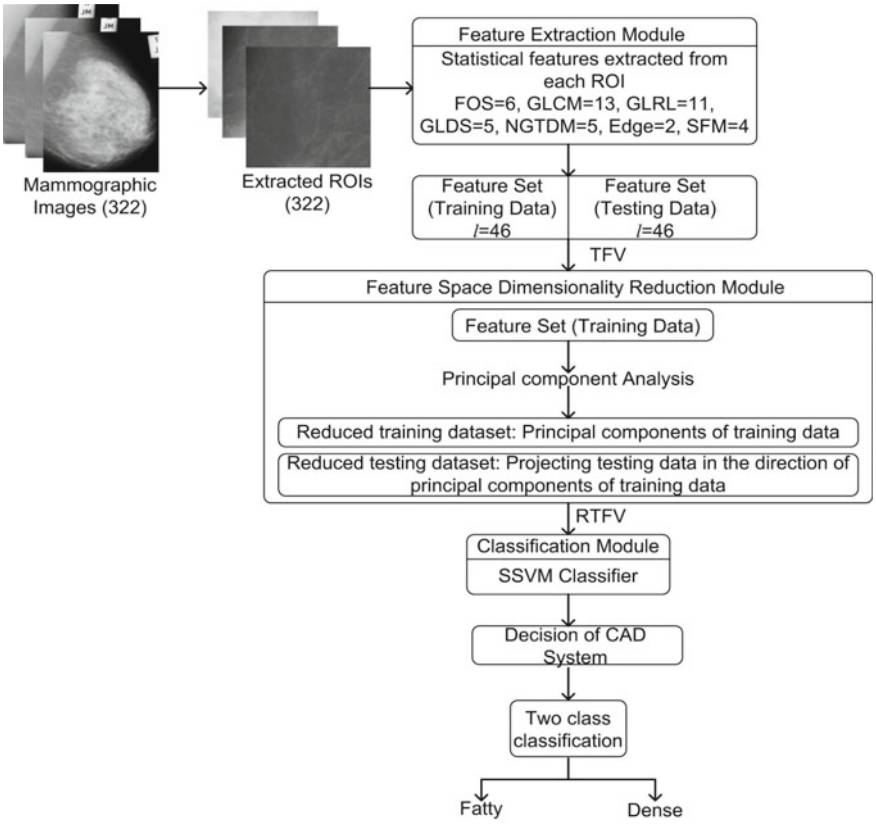

Fig. 8 Proposed SSVM based CAD system design for two-class breast tissue density classification

4 Conclusion

From the rigorous experiments carried out in the present work, it can be observed that for two-class breast tissue density, PCA-SSVM based CAD system using first 10 PCs obtained by applying PCA to the TFV derived using statistical features yields highest OCA of 94.4 % using mammographic images. It could also be observed that the PCA-SVM based CAD system using first 4 PCs obtained by applying PCA to the TFV derived using statistical features yields highest OCA of 86.3 % for three-class breast tissue density classification using mammographic images. It can be concluded that statistical features are significant to account for the textural changes exhibited by the fatty and dense breast tissues. The proposed CAD system designs derived using the above results are shown in Figs. 8 and 9 for two-class and three-class breast tissue density classification, respectively.

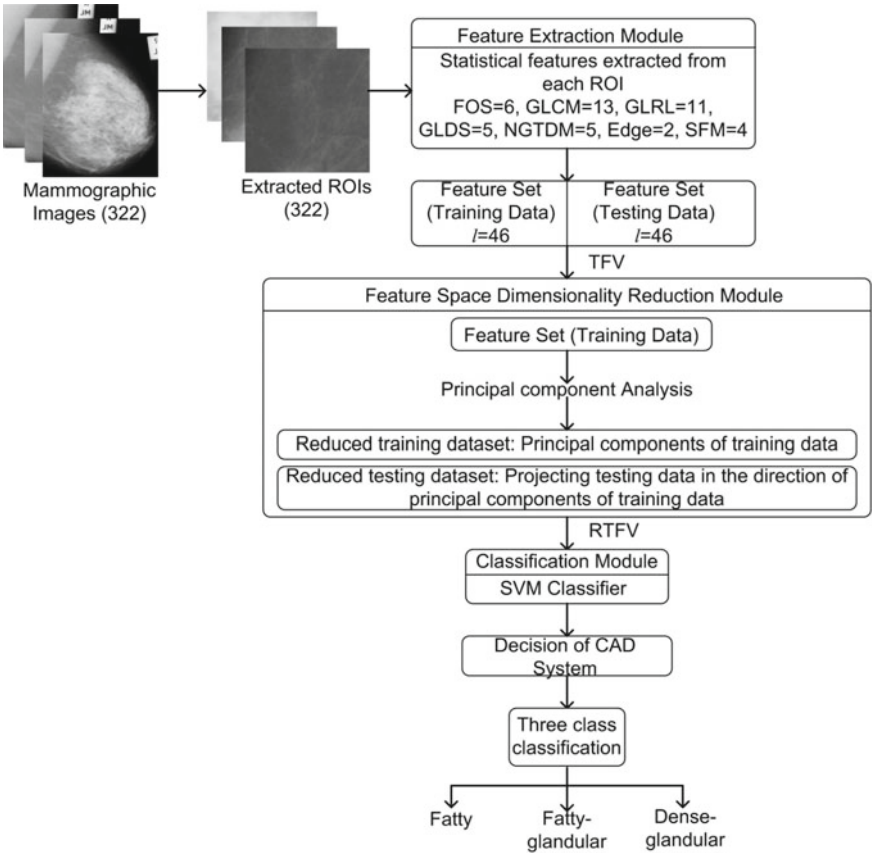

Fig. 9 Proposed CAD system design for three-class breast tissue density classification

The promising results obtained by the proposed CAD system designs indicate their usefulness to assist radiologists for characterization of breast tissue density during routine clinical practice.

References

1. Ganesan, K., Acharya, U.R., Chua, C.K., Min, L.C., Abraham, T.K., Ng, K.H.: Computer-aided breast cancer detection using mammograms: a review. IEEE Rev. Biomed. Eng. **6**, 77–98 (2013)
2. What is cancer? MNT Knowledge Center. http://www.medicalnewstoday.com/info/cancer-oncology/
3. Breast cancer awareness month in October, World Health Organisation, 2012. http://www.who.int/cancer/events/breast_cancer_month/en/
4. Cancer stats: key stats, Cancer Research UK. http://www.cancerresearchuk.org/cancer-info/cancerstats/keyfacts/
5. Globocan 2012: Estimated cancer incidence, mortality and prevalence worldwide, International Agency for Research on Cancer, 2012. http://globocan.iarc.fr/Default.aspx
6. Wolfe, J.N.: Breast patterns as an index of risk for developing breast cancer. Am. J. Roentgenol. **126**(6), 1130–1137 (1976)
7. Wolfe, J.N.: Risk for breast cancer development determined by mammographic parenchymal pattern. Cancer **37**(5), 2486–2492 (1976)
8. Boyd, N.F., Rommens, J.M., Vogt, K., Lee, V., Hopper, J.L., Yaffe, M.J., Paterson, A.D.: Mammographic breast density as an intermediate phenotype for breast cancer. Lancet Oncol. **6**(10), 798–808 (2005)
9. Boyd, N.F., Martin, L.J., Chavez, S., Gunasekara, A., Salleh, A., Melnichouk, O., Yaffe, M., Friedenreich, C., Minkin, S., Bronskill, M.: Breast Tissue composition and other risk factors for breast cancer in young women: a cross sectional study. Lancet Oncol. **10**(6), 569–580 (2009)
10. Boyd, N.F., Martin, L.J., Yaffe, M.J., Minkin, S.: Mammographic density and breast cancer risk: current understanding and future prospects. Breast Cancer Res. **13**(6), 223–235 (2011)
11. Boyd, N.F., Guo, H., Martin, L.J., Sun, L., Stone, J., Fishell, E., Jong, R.A., Hislop, G., Chiarelli, A., Minkin, S., Yaffe, M.J.: Mammographic density and the risk and detection of breast cancer. New Engl. J. Med. **356**(3), 227–236 (2007)
12. Vachon, C.M., Gils, C.H., Sellers, T.A., Ghosh, K., Pruthi, S., Brandt, K.R., Pankratz, V.S.: Mammographic density, breast cancer risk and risk prediction. Breast Cancer Res. **9**(6), 217–225 (2007)
13. Warren, R.: Hormones and mammographic breast density. Maturitas **49**(1), 67–78 (2004)
14. Al Mousa, D.S., Brennan, P.C., Ryan, E.A., Lee, W.B., Tan, J., Mello-Thomas, C.: How mammographic breast density affects radiologists' visual search patterns. Acad. Radiol. **21**(11), 1386–1393 (2014)
15. Boyd, N.F., Lockwood, G.A., Byng, J.W., Tritchler, D.L., Yaffe, M.J.: Mammographic densities and breast cancer risk. Cancer Epidemiol. Biomark. Prev. **7**(12), 1133–1144 (1998)
16. Papaevangelou, A., Chatzistergos, S., Nikita, K.S., Zografos, G.: Breast density: computerized analysis on digitized mammograms. Hellenic J. Surg. **83**(3), 133–138 (2011)
17. Colin, C., Prince, V., Valette, P.J.: Can mammographic assessments lead to consider density as a risk factor for breast cancer? Eur. J. Radiol. **82**(3), 404–411 (2013)
18. Zhou, C., Chan, H.P., Petrick, N., Helvie, M.A., Goodsitt, M.M., Sahiner, B., Hadjiiski, L.M.: Computerized image analysis: estimation of breast density on mammograms. Med. Phys. **28**, 1056–1069 (2001)
19. Heine, J.J., Carton, M.J., Scott, C.G.: An automated approach for estimation of breast density. Cancer Epidemiol. Biomark. Prev. **17**(11), 3090–3097 (2008)

20. Huo, Z., Giger, M.L., Vyborny, C.J.: Computerized analysis of multiple-mammographic views: potential usefulness of special view mammograms in computer-aided diagnosis. IEEE Trans. Med. Imaging **20**(12), 1285–1292 (2001)
21. Jagannath, H.S., Virmani, J., Kumar, V.: Morphological enhancement of microcalcifications in digital mammograms. J. Inst. Eng. (India): Ser. B. **93**(3), 163–172 (2012)
22. Yaghjyan, L., Pinney, S.M., Mahoney, M.C., Morton, A.R., Buckholz, J.: Mammographic breast density assessment: a methods study. Atlas J. Med. Biol. Sci. **1**(1), 8–14 (2011)
23. Virmani, J., Kumar, V.: Quantitative evaluation of image enhancement techniques. In: Proceedings of International Conference on Biomedical Engineering and Assistive Technology (BEATS), pp. 1–8. IEEE Press, New York (2010)
24. Miller, P., Astley, A.: Classification of Breast tissue by texture analysis. Image Vis. Comput. **10**(5), 277–282 (1992)
25. Bovis, K., Singh, S.: Classification of mammographic breast density using a combined classifier paradigm. In: 4th International Workshop on Digital Mammography, pp. 1–4 (2002)
26. Castella, C., Kinkel, K., Eckstein, M.P., Sottas, P.E., Verdun, F.R., Bochud, F.: Semiautomatic mammographic parenchymal patterns classification using multiple statistical features. Acad. Radiol. **14**(12), 1486–1499 (2007)
27. Oliver, A., Freixenet, J., Marti, R., Pont, J., Perez, E., Denton, E.R.E., Zwiggelaar, R.: A novel breast tissue density classification methodology. IEEE Trans. Inf. Technol. Biomed. **12**, 55–65 (2008)
28. Mustra, M., Grgic, M., Delac, K.: Breast density classification using multiple feature selection. Auotomatika **53**(4), 362–372 (2012)
29. Sharma, V., Singh, S.: CFS-SMO based classification of breast density using multiple texture models. Med. Biol. Eng. Comput. **52**(6), 521–529 (2014)
30. Sharma, V., Singh, S.: Automated classification of fatty and dense mammograms. J. Med. Imaging Health Inf. **5**(3), 520–526 (7) (2015)
31. Kriti., Virmani, J., Dey, N., Kumar, V.: PCA-PNN and PCA-SVM based CAD systems for breast density classification. In: Hassanien, A.E., et al. (eds.) Applications of Intelligent Optimization in Biology and Medicine. vol. 96, pp. 159–180. Springer (2015)
32. Kriti., Virmani, J.: Breast tissue density classification using wavelet-based texture descriptors. In: Proceedings of the Second International Conference on Computer and Communication Technologies (IC3T-2015), vol. 3, pp. 539–546 (2015)
33. Blot, L., Zwiggelaar, R.: Background texture extraction for the classification of mammographic parenchymal patterns. In: Proceedings of Conference on Medical Image Understanding and Analysis, pp. 145–148 (2001)
34. Bosch, A., Munoz, X., Oliver, A., Marti, J.: Modelling and classifying breast tissue density in mammograms. computer vision and pattern recognition. In: IEEE Computer Society Conference, vol. 2, pp. 1552–1558. IEEE Press, New York (2006)
35. Muhimmah, I., Zwiggelaar, R.: Mammographic density classification using multiresolution histogram information. In: Proceedings of 5th International IEEE Special Topic Conference on Information Technology in Biomedicine (ITAB), pp. 1–6. IEEE Press, New York (2006)
36. Subashini, T.S., Ramalingam, V., Palanivel, S.: Automated assessment of breast tissue density in digital mammograms. Comput. Vis. Image Underst. **114**(1), 33–43 (2010)
37. Tzikopoulos, S.D., Mavroforakis, M.E., Georgiou, H.V., Dimitropoulos, N., Theodoridis, S.: a fully automated scheme for mammographic segmentation and classification based on breast density and asymmetry. Comput. Methods Programs Biomed. **102**(1), 47–63 (2011)
38. Li, J.B.: Mammographic image based breast tissue classification with kernel self-optimized fisher discriminant for breast cancer diagnosis. J. Med. Syst. **36**(4), 2235–2244 (2012)
39. Silva, W.R., Menotti, D.: Classification of mammograms by the breast composition. In: Proceedings of the 2012 International Conference on Image Processing, Computer Vision, and Pattern Recognition, pp. 1–6 (2012)
40. Karssemeijer, N.: Automated classification of parenchymal patterns in mammograms. Phys. Med. Biol. **43**(2), 365–378 (1998)

41. Wang, X.H., Good, W.F., Chapman, B.E., Chang, Y.H., Poller, W.R., Chang, T.S., Hardesty, L.A.: Automated assessment of the composition of breast tissue revealed on tissue-thickness-corrected mammography. Am. J. Roentgenol. **180**(1), 257–262 (2003)
42. Petroudi, S., Kadir T., Brady, M.: Automatic classification of mammographic parenchymal patterns: a statistical approach. In: Proceedings of 25th Annual International Conference of IEEE on Engineering in Medicine and Biology Society, pp. 798–801. IEEE Press, New York (2003)
43. Oliver, A., Freixenet, J., Bosch, A., Raba, D., Zwiggelaar, R.: Automatic classification of breast tissue. In: Maeques, J.S., et al. (eds.) Pattern Recognition and Image Analysis. LNCS, vol. 3523, pp. 431–438. Springer, Heidelberg (2005)
44. Li, H., Giger, M.L., Huo, Z., Olopade, O.I., Lan, L., Weber, B.L., Bonta, I.: Computerized analysis of mammographic parenchymal patterns for assessing breast cancer risk: effect of ROI size and location. Med. Phys. **31**(3), 549–555 (2004)
45. Suckling, J., Parker, J., Dance, D.R., Astley, S., Hutt, I., Boggis, C.R.M., Ricketts, I., Stamatakis, E., Cerneaz, N., Kok, S.L., Taylor, P., Betal, D., Savage, J.: The mammographic image analysis society digital mammogram database. In: Gale, A.G., et al. (eds.) Digital Mammography. LNCS, vol. 169, pp. 375–378. Springer, Heidelberg (1994)
46. Tang, J., Rangayyan, R.M., Xu, J., El Naqa, I., Yang, Y.: Computer-aided detection and diagnosis of breast cancer with mammography: recent advances. IEEE Trans. Inf.Technol. Biomed. **13**(2), 236–251 (2009)
47. Tagliafico, A., Tagliafico, G., Tosto, S., Chiesa, F., Martinoli, C., Derechi, L.E., Calabrese, M.: Mammographic density estimation: comparison among BI-RADS categories, a semi-automated software and a fully automated one. The Breast **18**(1), 35–40 (2009)
48. Doi, K.: Computer-aided diagnosis in medical imaging: historical review, current status, and future potential. Comput. Med. Imaging Graph. **31**(4–5), 198–211 (2007)
49. Doi, K., MacMahon, H., Katsuragawa, S., Nishikawa, R.M., Jiang, Y.: Computer-aided diagnosis in radiology: potential and pitfalls'. Eur. J. Radiol. **31**(2), 97–109 (1997)
50. Giger, M.L., Doi, K., MacMahon, H., Nishikawa, R.M., Hoffmann, K.R., Vyborny, C.J., Schmidt, R.A., Jia, H., Abe, K., Chen, X., Kano, A., Katsuragawa, S., Yin, F.F., Alperin, N., Metz, C.E., Behlen, F.M., Sluis, D.: An intelligent workstation for computer-aided diagnosis. Radiographics **13**(3), 647–656 (1993)
51. Hui, L., Giger, M.L., Olopade, O.I., Margolis, A., Lan, L., Bonta, I.: Computerized texture analysis of mammographic parenchymal patterns of digitized mammograms. Int. Congr. Ser. **1268**, 878–881 (2004)
52. Kumar, I., Virmani, J., Bhadauria, H.S.: A review of breast density classification methods. In: Proceedings of 2nd IEEE International Conference on Computing for Sustainable Global Development. IndiaCom-2015, pp. 1960–1967. IEEE Press, New York (2015)
53. Tourassi, G.D.: Journey toward computer aided diagnosis: role of image texture analysis. Radiology **213**(2), 317–320 (1999)
54. Virmani, J., Kumar, V., Kalra, N., Khandelwal, N.: Prediction of cirrhosis from liver ultrasound B-Mode images based on laws' mask analysis. In: Proceedings of the IEEE International Conference on Image Information Processing. ICIIP-2011, pp. 1–5. IEEE Press, New York (2011)
55. Virmani, J., Kumar, V., Kalra, N., Khandelwal, N.: Neural network ensemble based CAD system for focal liver lesions from B-Mode ultrasound. J. Digit. Imaging **27**(4), 520–537 (2014)
56. Zhang, G., Wang, W., Moon, J., Pack, J.K., Jean, S.: A review of breast tissue classification in mammograms. In: Proceedings of ACM Symposium on Research in Applied Computation, pp. 232–237 (2011)
57. Chan, H.P., Doi, K., Vybrony, C.J., Schmidt, R.A., Metz, C., Lam, K.L., Ogura, T., Wu, Y., MacMahon, H.: Improvement in radiologists' detection of clustered micro-calcifications on mammograms: the potential of computer-aided diagnosis. Instigative Radiol. **25**(10), 1102–1110 (1990)

58. Virmani, J., Kumar, V., Kalra, N., Khandelwal, N.: Prediction of liver cirrhosis based on multiresolution texture descriptors from B-Mode ultrasound. Int. J. Convergence Comput. **1**(1), 19–37 (2013)
59. Virmani, J., Kumar, V., Kalra, N., Khandelwal, N.: A rapid approach for prediction of liver cirrhosis based on first order statistics. In: Proceedings of the IEEE International Conference on Multimedia. Signal Processing and Communication Technologies, pp. 212–215. IEEE Press, New York (2011)
60. Virmani, J., Kumar, V., Kalra, N., Khandelwal, N.: Prediction of cirrhosis based on singular value decomposition of gray level co-occurrence matrix and a neural network classifier. In: Proceedings of Development in E-systems Engineering (DESE-2011), pp. 146–151 (2011)
61. Vasantha, M., Subbiah Bharathi, V., Dhamodharan, R.: Medical image feature extraction, selection and classification. Int. J. Eng. Sci. Technol. **2**, 2071–2076 (2010)
62. Mohanaiah, P., Sathyanarayanam, P., Gurukumar, L.: Image texture feature extraction using GLCM approach. Int. J. Sci. Res. Publ. **3**(5), 1–5 (2013)
63. Xu, D.H., Kurani, A.S., Furst, J.D., Raicu, D.S.: Run-length encoding for volumetric texture. Heart **27**, 25–30 (2004)
64. Albregtsen, F.: Statistical texture measures computed from gray level run length matrices. Image **1**, 3–8 (1995)
65. Castellano, G., Bonilha, L., Li, L.M., Cendes, F.: Texture analysis of medical images. Clin. Radiol. **59**, 1061–1069 (2004)
66. Amadasun, M., King, R.: Textural features corresponding to textural properties. IEEE Trans. Syst. Man Cybern. **19**, 1264–1274 (1989)
67. Weszka, J.S., Dyer, C.R., Rosenfeld, A.: A comparative study of texture measures for terrain classification. IEEE Trans. Syst. Man Cybern. **6**(4), 269–285 (1976)
68. Kim, J.K., Park, H.W.: Statistical textural features for detection of microcalcifications in digitized mammograms. IEEE Trans. Med. Imaging **18**(3), 231–238 (1999)
69. Kumar, I., Bhadauria, H.S., Virmani, J., Rawat, J.: Reduction of speckle noise from medical images using principal component analysis image fusion. In: Proceedings of 9th International Conference on Industrial and Information Systems, pp. 1–6. IEEE Press, New York (2014)
70. Romano, R., Acernese, F., Canonico, R., Giordano, G., Barone, F.: A principal components algorithm for spectra normalization. Int. J. Biomed. Eng. Technol. **13**(4), 357–369 (2013)
71. Amendolia, S.R., Cossu, G., Ganadu, M.L., Galois, B., Masala, G.L., Mura, G.M.: A comparative study of k-nearest neighbor, support vector machine and multi-layer perceptron for thalassemia screening. Chemometr. Intell. Lab. Syst. **69**(1–2), 13–20 (2003)
72. Virmani, J., Kumar, V., Kalra, N., Khandelwal, N.: A comparative study of computer-aided classification systems for focal hepatic lesions from B-Mode ultrasound. J. Med. Eng. Technol. **37**(44), 292–306 (2013)
73. Yazdani, A., Ebrahimi, T., Hoffmann, U.: Classification of EEG signals using dempster shafer theory and a k-nearest neighbor classifier. In: Proceedings of 4th International IEEE EMBS Conference on Neural Engineering, pp. 327–330. IEEE Press, New York (2009)
74. Wu, Y., Ianakiev, K., Govindaraju, V.: Improved kNN classification. Pattern Recogn. **35**(10), 2311–2318 (2002)
75. Specht, D.F.: Probabilistic neural networks. Neural Netw. **1**, 109–118 (1990)
76. Specht, D.F., Romsdahl, H.: Experience with adaptive probabilistic neural network and adaptive general regression neural network. In: Proceedings of the IEEE International Conference on Neural Networks, pp. 1203–1208. IEEE Press, New York (1994)
77. Georgiou, V.L., Pavlidis, N.G., Parsopoulos, K.E., Vrahatis, M.N.: Optimizing the performance of probabilistic neural networks in a bioinformatics task. In: Proceedings of the EUNITE 2004 Conference, pp. 34–40 (2004)
78. Chang, C.C., Lin, C.J.: LIBSVM, a library of support vector machines. ACM Trans. Intell. Syst. Technol. **2**(3), 27–65 (2011)
79. Virmani, J., Kumar, V., Kalra, N., Khandelwal, N.: PCA-SVM based CAD system for focal liver lesion using B-Mode ultrasound images. Defence Sci. J. **63**(5), 478–486 (2013)

80. Virmani, J., Kumar, V., Kalra, N., Khandelwal, N.: SVM-based characterization of liver cirrhosis by singular value decomposition of GLCM matrix. Int. J. Artif. Intell. Soft Comput. **3**(3), 276–296 (2013)
81. Hassanien, A.E., Bendary, N.E., Kudelka, M., Snasel, V.: Breast cancer detection and classification using support vector machines and pulse coupled neural network. In: Proceedings of 3rd International Conference on Intelligent Human Computer Interaction (IHCI 2011), pp. 269–279 (2011)
82. Azar, A.T., El-Said, S.A.: Performance analysis of support vector machine classifiers in breast cancer mammography recognition. Neural Comput. Appl. **24**, 1163–1177 (2014)
83. Virmani, J., Kumar, V., Kalra, N., Khandelwal, N.: SVM-based characterization of liver ultrasound images using wavelet packet texture descriptors. J. Digit. Imaging **26**(3), 530–543 (2013)
84. Purnami, S.W., Embong, A., Zain, J.M., Rahayu, S.P.: A new smooth support vector machine and its applications in diabetes disease diagnosis. J. Comput. Sci. **5**(12), 1003–1008 (2009)
85. Lee, Y.J., Mangasarian, O.L.: SSVM: a smooth support vector machine for classification. Comput. Optim. Appl. **20**, 5–22 (2001)
86. Lee, Y.J., Mangasarian, O.L.: SSVM toolbox. http://research.cs.wisc.edu/dmi/svm/ssvm/